

Enhanced strange baryon production in Au+Au collisions compared to $p+p$ at $\sqrt{s_{NN}}=200$ GeV

B.I. Abelev,¹⁰ M.M. Aggarwal,³² Z. Ahammed,⁴⁷ B.D. Anderson,²¹ D. Arkhipkin,¹⁴ G.S. Averichev,¹³ Y. Bai,³⁰ J. Balewski,¹⁸ O. Barannikova,¹⁰ L.S. Barnby,² J. Baudot,¹⁹ S. Baumgart,⁵² D.R. Beavis,³ R. Bellwied,⁵⁰ F. Benedosso,³⁰ R.R. Betts,¹⁰ S. Bhardwaj,³⁷ A. Bhasin,²⁰ A.K. Bhati,³² H. Bichsel,⁴⁹ J. Bielcik,¹² J. Bielcikova,¹² L.C. Bland,³ S-L. Blyth,²⁴ M. Bombara,² B.E. Bonner,³⁸ M. Botje,³⁰ J. Bouchet,⁴² E. Braidot,³⁰ A.V. Brandin,²⁸ S. Bueltmann,³ T.P. Burton,² M. Bystersky,¹² X.Z. Cai,⁴¹ H. Caines,⁵² M. Calderón de la Barca Sánchez,⁶ J. Callner,¹⁰ O. Catu,⁵² D. Cebra,⁶ M.C. Cervantes,⁴³ Z. Chajecski,³¹ P. Chaloupka,¹² S. Chattopadhyay,⁴⁷ H.F. Chen,⁴⁰ J.H. Chen,⁴¹ J.Y. Chen,⁵¹ J. Cheng,⁴⁵ M. Cherney,¹¹ A. Chikanian,⁵² K.E. Choi,³⁶ W. Christie,³ S.U. Chung,³ R.F. Clarke,⁴³ M.J.M. Coddington,⁴³ J.P. Coffin,¹⁹ T.M. Cormier,⁵⁰ M.R. Cosentino,³⁹ J.G. Cramer,⁴⁹ H.J. Crawford,⁵ D. Das,⁶ S. Dash,¹⁶ M. Daugherty,⁴⁴ M.M. de Moura,³⁹ T.G. Dedovich,¹³ M. DePhillips,³ A.A. Derevschikov,³⁴ R. Derradi de Souza,⁸ L. Didenko,³ T. Dietel,¹⁵ P. Djawotho,¹⁸ S.M. Dogra,²⁰ X. Dong,²⁴ J.L. Drachenberg,⁴³ J.E. Draper,⁶ F. Du,⁵² J.C. Dunlop,³ M.R. Dutta Mazumdar,⁴⁷ W.R. Edwards,²⁴ L.G. Efimov,¹³ E. Elhalhuli,² V. Emelianov,²⁸ J. Engelage,⁵ G. Eppley,³⁸ B. Erazmus,⁴² M. Estienne,¹⁹ L. Eun,³³ P. Fachini,³ R. Fatemi,²² J. Fedorisin,¹³ A. Feng,⁵¹ P. Filip,¹⁴ E. Finch,⁵² V. Fine,³ Y. Fisyak,³ J. Fu,⁵¹ C.A. Gagliardi,⁴³ L. Gaillard,² M.S. Ganti,⁴⁷ E. Garcia-Solis,¹⁰ V. Ghazikhanian,⁷ P. Ghosh,⁴⁷ Y.N. Gorbunov,¹¹ A. Gordon,³ O. Grebenyuk,³⁰ D. Grosnick,⁴⁶ B. Grube,³⁶ S.M. Guertin,⁷ K.S.F.F. Guimaraes,³⁹ A. Gupta,²⁰ N. Gupta,²⁰ W. Guryn,³ B. Haag,⁶ T.J. Hallman,³ A. Hamed,⁴³ J.W. Harris,⁵² W. He,¹⁸ M. Heinz,⁵² T.W. Henry,⁴³ S. Heppelmann,³³ B. Hippolyte,¹⁹ A. Hirsch,³⁵ E. Hjort,²⁴ A.M. Hoffman,²⁵ G.W. Hoffmann,⁴⁴ D.J. Hofman,¹⁰ R.S. Hollis,¹⁰ M.J. Horner,²⁴ H.Z. Huang,⁷ E.W. Hughes,⁴ T.J. Humanic,³¹ G. Igo,⁷ A. Iordanova,¹⁰ P. Jacobs,²⁴ W.W. Jacobs,¹⁸ P. Jakl,¹² F. Jin,⁴¹ P.G. Jones,² E.G. Judd,⁵ S. Kabana,⁴² K. Kajimoto,⁴⁴ K. Kang,⁴⁵ J. Kapitan,¹² M. Kaplan,⁹ D. Keane,²¹ A. Kechechyan,¹³ D. Kettler,⁴⁹ V.Yu. Khodyrev,³⁴ J. Kiryluk,²⁴ A. Kisiel,³¹ S.R. Klein,²⁴ A.G. Knospe,⁵² A. Kocoloski,²⁵ D.D. Koetke,⁴⁶ T. Kollegger,¹⁵ M. Kopytine,²¹ L. Kotchenda,²⁸ V. Kouchpil,¹² K.L. Kowalik,²⁴ P. Kravtsov,²⁸ V.I. Kravtsov,³⁴ K. Krueger,¹ C. Kuhn,¹⁹ A. Kumar,³² L. Kumar,³² P. Kurnadi,⁷ M.A.C. Lamont,³ J.M. Landgraf,³ S. Lange,¹⁵ S. LaPointe,⁵⁰ F. Laue,³ J. Lauret,³ A. Lebedev,³ R. Lednicky,¹⁴ C-H. Lee,³⁶ M.J. LeVine,³ C. Li,⁴⁰ Q. Li,⁵⁰ Y. Li,⁴⁵ G. Lin,⁵² X. Lin,⁵¹ S.J. Lindenbaum,²⁹ M.A. Lisa,³¹ F. Liu,⁵¹ H. Liu,⁴⁰ J. Liu,³⁸ L. Liu,⁵¹ T. Ljubicic,³ W.J. Llope,³⁸ R.S. Longacre,³ W.A. Love,³ Y. Lu,⁴⁰ T. Ludlam,³ D. Lynn,³ G.L. Ma,⁴¹ J.G. Ma,⁷ Y.G. Ma,⁴¹ D.P. Mahapatra,¹⁶ R. Majka,⁵² L.K. Mangotra,²⁰ R. Manweiler,⁴⁶ S. Margetis,²¹ C. Markert,⁴⁴ H.S. Matis,²⁴ Yu.A. Matulenko,³⁴ T.S. McShane,¹¹ A. Meschanin,³⁴ J. Millane,²⁵ M.L. Miller,²⁵ N.G. Minaev,³⁴ S. Mioduszewski,⁴³ A. Mischke,³⁰ J. Mitchell,³⁸ B. Mohanty,⁴⁷ D.A. Morozov,³⁴ M.G. Munhoz,³⁹ B.K. Nandi,¹⁷ C. Nattrass,⁵² T.K. Nayak,⁴⁷ J.M. Nelson,² C. Nepali,²¹ P.K. Netrakanti,³⁵ M.J. Ng,⁵ L.V. Nogach,³⁴ S.B. Nurushev,³⁴ G. Odyniec,²⁴ A. Ogawa,³ H. Okada,³ V. Okorokov,²⁸ D. Olson,²⁴ M. Pachr,¹² S.K. Pal,⁴⁷ Y. Panebratsev,¹³ A.I. Pavlinov,⁵⁰ T. Pawlak,⁴⁸ T. Peitzmann,³⁰ V. Perevoztchikov,³ C. Perkins,⁵ W. Peryt,⁴⁸ S.C. Phatak,¹⁶ M. Planinic,⁵³ J. Pluta,⁴⁸ N. Poljak,⁵³ N. Porile,³⁵ A.M. Poskanzer,²⁴ M. Potekhin,³ B.V.K.S. Potukuchi,²⁰ D. Prindle,⁴⁹ C. Pruneau,⁵⁰ N.K. Pruthi,³² J. Putschke,⁵² I.A. Qattan,¹⁸ R. Raniwala,³⁷ S. Raniwala,³⁷ R.L. Ray,⁴⁴ D. Relyea,⁴ A. Ridiger,²⁸ H.G. Ritter,²⁴ J.B. Roberts,³⁸ O.V. Rogachevskiy,¹³ J.L. Romero,⁶ A. Rose,²⁴ C. Roy,⁴² L. Ruan,³ M.J. Russcher,³⁰ V. Rykov,²¹ R. Sahoo,⁴² I. Sakrejda,²⁴ T. Sakuma,²⁵ S. Salur,⁵² J. Sandweiss,⁵² M. Sarsour,⁴³ J. Schambach,⁴⁴ R.P. Scharenberg,³⁵ N. Schmitz,²⁶ J. Seger,¹¹ I. Selyuzhenkov,⁵⁰ P. Seyboth,²⁶ A. Shabetai,¹⁹ E. Shahaliev,¹³ M. Shao,⁴⁰ M. Sharma,⁵⁰ X-H. Shi,⁴¹ E.P. Sichtermann,²⁴ F. Simon,²⁶ R.N. Singaraju,⁴⁷ M.J. Skoby,³⁵ N. Smirnov,⁵² R. Snellings,³⁰ P. Sorensen,³ J. Sowinski,¹⁸ J. Speltz,¹⁹ H.M. Spinka,¹ B. Srivastava,³⁵ A. Stadnik,¹³ T.D.S. Stanislaus,⁴⁶ D. Staszak,⁷ R. Stock,¹⁵ M. Strikhanov,²⁸ B. Stringfellow,³⁵ A.A.P. Suaide,³⁹ M.C. Suarez,¹⁰ N.L. Subba,²¹ M. Sumbera,¹² X.M. Sun,²⁴ Z. Sun,²³ B. Surrow,²⁵ T.J.M. Symons,²⁴ A. Szanto de Toledo,³⁹ J. Takahashi,⁸ A.H. Tang,³ Z. Tang,⁴⁰ T. Tarnowsky,³⁵ D. Thein,⁴⁴ J.H. Thomas,²⁴ J. Tian,⁴¹ A.R. Timmins,² S. Timoshenko,²⁸ M. Tokarev,¹³ T.A. Trainor,⁴⁹ V.N. Tram,²⁴ A.L. Trattner,⁵ S. Trentalange,⁷ R.E. Tribble,⁴³ O.D. Tsai,⁷ J. Ulery,³⁵ T. Ullrich,³ D.G. Underwood,¹ G. Van Buren,³ N. van der Kolk,³⁰ M. van Leeuwen,²⁴ A.M. Vander Molen,²⁷ R. Varma,¹⁷ G.M.S. Vasconcelos,⁸ I.M. Vasilevski,¹⁴ A.N. Vasiliev,³⁴ R. Vernet,¹⁹ F. Videbaek,³ S.E. Vigdor,¹⁸ Y.P. Viyogi,¹⁶ S. Vokal,¹³ S.A. Voloshin,⁵⁰ M. Wada,⁴⁴ W.T. Waggoner,¹¹ F. Wang,³⁵ G. Wang,⁷ J.S. Wang,²³ Q. Wang,³⁵ X. Wang,⁴⁵ X.L. Wang,⁴⁰ Y. Wang,⁴⁵ J.C. Webb,⁴⁶ G.D. Westfall,²⁷ C. Whitten Jr.,⁷ H. Wieman,²⁴ S.W. Wissink,¹⁸ R. Witt,⁵² J. Wu,⁴⁰ Y. Wu,⁵¹ N. Xu,²⁴ Q.H. Xu,²⁴ Z. Xu,³ P. Yepes,³⁸

I-K. Yoo,³⁶ Q. Yue,⁴⁵ M. Zawisza,⁴⁸ H. Zbroszczyk,⁴⁸ W. Zhan,²³ H. Zhang,³ S. Zhang,⁴¹ W.M. Zhang,²¹
 Y. Zhang,⁴⁰ Z.P. Zhang,⁴⁰ Y. Zhao,⁴⁰ C. Zhong,⁴¹ J. Zhou,³⁸ R. Zoukarneev,¹⁴ Y. Zoukarneeva,¹⁴ and J.X. Zuo⁴¹
 (STAR Collaboration)

- ¹Argonne National Laboratory, Argonne, Illinois 60439
²University of Birmingham, Birmingham, United Kingdom
³Brookhaven National Laboratory, Upton, New York 11973
⁴California Institute of Technology, Pasadena, California 91125
⁵University of California, Berkeley, California 94720
⁶University of California, Davis, California 95616
⁷University of California, Los Angeles, California 90095
⁸Universidade Estadual de Campinas, Sao Paulo, Brazil
⁹Carnegie Mellon University, Pittsburgh, Pennsylvania 15213
¹⁰University of Illinois at Chicago, Chicago, Illinois 60607
¹¹Creighton University, Omaha, Nebraska 68178
¹²Nuclear Physics Institute AS CR, 250 68 Řež/Prague, Czech Republic
¹³Laboratory for High Energy (JINR), Dubna, Russia
¹⁴Particle Physics Laboratory (JINR), Dubna, Russia
¹⁵University of Frankfurt, Frankfurt, Germany
¹⁶Institute of Physics, Bhubaneswar 751005, India
¹⁷Indian Institute of Technology, Mumbai, India
¹⁸Indiana University, Bloomington, Indiana 47408
¹⁹Institut de Recherches Subatomiques, Strasbourg, France
²⁰University of Jammu, Jammu 180001, India
²¹Kent State University, Kent, Ohio 44242
²²University of Kentucky, Lexington, Kentucky, 40506-0055
²³Institute of Modern Physics, Lanzhou, China
²⁴Lawrence Berkeley National Laboratory, Berkeley, California 94720
²⁵Massachusetts Institute of Technology, Cambridge, MA 02139-4307
²⁶Max-Planck-Institut für Physik, Munich, Germany
²⁷Michigan State University, East Lansing, Michigan 48824
²⁸Moscow Engineering Physics Institute, Moscow Russia
²⁹City College of New York, New York City, New York 10031
³⁰NIKHEF and Utrecht University, Amsterdam, The Netherlands
³¹Ohio State University, Columbus, Ohio 43210
³²Panjab University, Chandigarh 160014, India
³³Pennsylvania State University, University Park, Pennsylvania 16802
³⁴Institute of High Energy Physics, Protvino, Russia
³⁵Purdue University, West Lafayette, Indiana 47907
³⁶Pusan National University, Pusan, Republic of Korea
³⁷University of Rajasthan, Jaipur 302004, India
³⁸Rice University, Houston, Texas 77251
³⁹Universidade de Sao Paulo, Sao Paulo, Brazil
⁴⁰University of Science & Technology of China, Hefei 230026, China
⁴¹Shanghai Institute of Applied Physics, Shanghai 201800, China
⁴²SUBATECH, Nantes, France
⁴³Texas A&M University, College Station, Texas 77843
⁴⁴University of Texas, Austin, Texas 78712
⁴⁵Tsinghua University, Beijing 100084, China
⁴⁶Valparaiso University, Valparaiso, Indiana 46383
⁴⁷Variable Energy Cyclotron Centre, Kolkata 700064, India
⁴⁸Warsaw University of Technology, Warsaw, Poland
⁴⁹University of Washington, Seattle, Washington 98195
⁵⁰Wayne State University, Detroit, Michigan 48201
⁵¹Institute of Particle Physics, CCNU (HZNU), Wuhan 430079, China
⁵²Yale University, New Haven, Connecticut 06520
⁵³University of Zagreb, Zagreb, HR-10002, Croatia

We report on the observed differences in production rates of strange and multi-strange baryons in Au+Au collisions at $\sqrt{s_{NN}} = 200$ GeV compared to $p+p$ interactions at the same energy. The strange baryon yields in Au+Au collisions, when scaled down by the number of participating nucleons, are enhanced relative to those measured in $p+p$ reactions. The enhancement observed increases with the strangeness content of the baryon, and increases for all strange baryons with collision centrality. The enhancement is qualitatively similar to that observed at lower collision energy $\sqrt{s_{NN}} = 17.3$

GeV. The previous observations are for the bulk production, while at intermediate p_T , $1 < p_T < 4$ GeV/c, the strange baryons even exceed binary scaling from $p+p$ yields.

PACS numbers: 25.75.-q,25.75.Dw,25.75.Nq,12.40.Ee

One of the aims of studying relativistic heavy ion collisions is to observe how matter behaves at extremes of temperature and/or density. The energy densities in the medium produced by these collisions are far from that of ground state nuclear matter. Ultimately we hope to determine if they are sufficiently high to create a system where the degrees of freedoms are those of quarks and gluons, a state called the Quark-Gluon Plasma (QGP). By comparing the particles produced in A+A to those from $p+p$ collisions, in which a QGP phase is not expected, we can gain insight into the properties of the medium.

Strange particles are of particular interest since the initial strangeness content of the colliding nuclei is very small and there is no net strangeness. This means that all strange hadrons must be formed in the matter produced. Originally, it was proposed that strangeness production would be increased due to the formation of a QGP compared to that from a hadron gas [1]. This enhancement is due to the high production rate of $gg \rightarrow s\bar{s}$ in a QGP, a process absent in the hadronic state. The subsequent hadronization of these (anti)strange quarks results in a significant increase in strange particle production, thus signaling a plasma was formed.

The concept of enhanced strangeness production in the QGP can be recast in the language of statistical mechanics. A Grand Canonical Ensemble limit is likely only to be reached in the high multiplicity of heavy ion reactions. If this is the case, any measured enhancement is really a phase space suppression in $p+p$ reactions that is removed in the heavy ion case. This lack of available phase space in small systems, such as those from $p+p$ collisions, requires a Canonical ensemble to be used which results in a suppression of strangeness production when scaled to the appropriate volume [2, 3]. However, there is no a priori method for directly calculating this volume and thus the authors make the simplest hypothesis and assume that the volume is linearly proportional to the number of collision participants, $\langle N_{part} \rangle$. The degree of suppression increases with the strange quark content of the particle. For sufficiently large volumes, the system is thermalized, the phase space suppression effects disappear, and the yields scale linearly with the volume, i.e. $\langle N_{part} \rangle$. Initial measurements from the SPS suggested such a linear $\langle N_{part} \rangle$ scaling [4]. However, it is not observed at RHIC [5] or in the more recent SPS results [6].

While the observables mentioned above are sensitive to the bulk of the produced particles with momenta below 2 GeV/c, further important information can be extracted from intermediate and high p_T particles. At RHIC, hadrons are suppressed at intermediate to high p_T

when compared to binary-scaled $p+p$ data at the same energy [7]. This effect is attributed to the energy loss of partons as they traverse the hot and dense medium produced [8, 9]. Measurements using identified particles help shed light on the details of the energy loss mechanism.

In this paper we present further analysis of the high statistics measurements from $p+p$ and Au+Au collisions at $\sqrt{s_{NN}}=200$ GeV for strange and multi-strange baryon production at mid-rapidity as reported by the STAR collaboration at RHIC [5, 11]. Details of the STAR experiment are in [10]. Specific details of the trigger and detectors used to collect the data reported here can be found in [5, 11] and references therein. The Au+Au event sample consisted of 1.5×10^6 central collision triggers and 1.6×10^6 minimum bias triggers. The $p+p$ results are from 6×10^6 minimum bias events. Particle identification is via the reconstruction of the charged daughter decay particles in the Time Projection Chamber. The decay channels used are $\Lambda \rightarrow p + \pi^-$, $\Xi^- \rightarrow \Lambda + \pi^- \rightarrow p + \pi^- + \pi^-$ and $\Omega^- \rightarrow \Lambda + K^- \rightarrow p + \pi^- + K^-$ plus the charge conjugates for the anti-particle decays.

After cuts, to reduce random combinatorics, parent particles were selected if the calculated invariant mass fell within 3σ around the peak after background subtraction. The data were corrected, as a function of p_T , for efficiency and detector acceptance. Monte-Carlo studies showed that the corrections were constant as a function of rapidity over the measured regions. Further details of these reconstruction and correction techniques can be found in [5, 11] and references therein. Several contributions to the systematic uncertainty of particle yields were studied: detector simulation and efficiency calculations, inhomogeneities of the detector responses, pile-up effects and the extrapolation of the data fits to zero p_T . In $p+p$ collisions an additional normalization error due to varying beam luminosity and trigger efficiencies of $\sim 4\%$ is included. The Λ yields were corrected for feed-down from multi-strange baryons using the measured spectra, the correction was of the order of 15%.

For each species, i , the yield enhancement, $E(i)$, above that expected from $\langle N_{part} \rangle$ scaling was calculated using:

$$E(i) = \frac{Yield^{AA}(i)\langle N_{part}^{NN} \rangle}{Yield^{NN}(i)\langle N_{part}^{AA} \rangle} \quad (1)$$

Fig. 1 shows $E(i)$ as a function of $\langle N_{part} \rangle$, the inclusive proton data illustrate the effects for non-strange baryons [12]. Mid-rapidity hyperon yields measured as a function of centrality in Au+Au [5] and $p+p$ [11] collisions were used. The number of participants, $\langle N_{part} \rangle$, and the number of binary collisions, $\langle N_{bin} \rangle$, were esti-

mated via a Monte-Carlo Glauber calculation [13, 14]. Since the $p+p$ data were recorded with a trigger that was only sensitive to the non-singly diffractive (NSD) part of the total inelastic cross-section, all $p+p$ yields have been corrected by $\sigma_{NSD}^{NN}/\sigma_{inel}^{NN}$, ($=30/42$), to obtain the total invariant cross-sections.

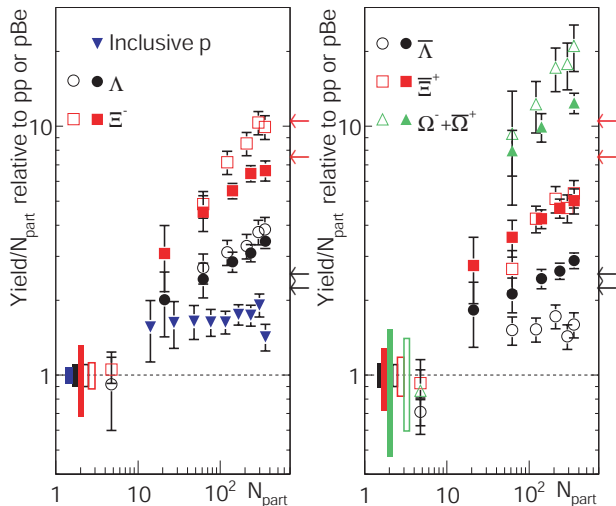


FIG. 1: (color online) Mid-rapidity $E(i)$ as a function of $\langle N_{part} \rangle$ for Λ , $\bar{\Lambda}$ ($|y| < 1.0$), Ξ^- , $\bar{\Xi}^+$, $\Omega^- + \bar{\Omega}^+$ ($|y| < 0.75$) and inclusive p ($|y| < 0.5$). Boxes at unity show statistical and systematical uncertainties combined in the $p+p$ ($p+Be$) data. Error bars on the data points represent those from the heavy-ions. The solid markers are for Au+Au at $\sqrt{s_{NN}}=200$ GeV and the open symbols for Pb+Pb ($|y| < 0.5$) at $\sqrt{s_{NN}}=17.3$ GeV [4]. The arrows on the right axes mark the predictions from a GC formalism model when varying T from 165 MeV ($E(\Xi^-)=10.7$, $E(\Lambda)=2.6$) to 170 MeV ($E(\Xi^-)=7.5$, $E(\Lambda)=2.2$). The red arrows indicate the predictions for Ξ and the black arrows those for Λ , see text for details [16].

It can be seen that there is an enhancement in the yields over that expected from $\langle N_{part} \rangle$ scaling for all the particles presented. Since the proton yields are not corrected for feed-down, which is predominantly from the Λ and Σ , the p measurement is actually a sum of the primary protons and those from secondary decays. The integrated $\Lambda + \Sigma^0$ over inclusive p ratio varies from 30 to 40 % for the $p+p$ and Au+Au collisions respectively. If only primary protons were measured $E(\text{proton})$ would be closer to unity. A hierarchy in the scale of enhancements, which grows with increased strangeness of the baryon, is observed. This trend is predicted by Grand Canonical (GC) ensemble approaches, as is the fact that the $E(i)$ values for each baryon/anti-baryon pair are similar in shape [2]. The difference in the scale of the enhancements for baryon and anti-baryon, especially at the SPS, is due to the existence of a non-zero net-baryon number. However, the ratio of $E(\text{anti-baryon})$ to $E(\text{baryon})$ varies as a function of $\langle N_{part} \rangle$ at the SPS, possibly sig-

nifying different production/annihilation mechanisms for (anti)particles at the SPS compared to at RHIC. For instance the net- Λ yields at the SPS, can be successfully described via multiple interactions of the projectile nuclei [15]. This effect is expected to be less significant at RHIC. It is also interesting to note that the measured enhancements for the Λ , anti(Ξ), and Ω at RHIC are the same, within errors, as those calculated from the mid-rapidity SPS data (open symbols in Fig. 1) despite an order of magnitude increase in the collision energies. Theoretical predictions using the GC ensemble approach predict a significant decrease in all the (anti)baryon enhancements with collision energy [2]. A GC model, with a chemical freeze-out temperature of $T=165$ MeV and a baryon chemical potential, $\mu_b = 29$ MeV calculates enhancements of $E(\Xi^-)=10.7$ and $E(\Lambda)=2.6$ for the most central Au+Au events at $\sqrt{s_{NN}}=200$ GeV [16]. These enhancement calculations cannot consistently describe the (anti) Ξ and the (anti) Λ enhancements. However, the scales of the enhancements are very sensitive to the assumed freeze-out temperature and if $T=170$ MeV is used $E(\Xi^-)=7.5$ and $E(\Lambda)=2.2$.

While the measured enhancements are approximately constant for the inclusive protons they are clearly not for the Λ , Ξ , and Ω ; this is again counter to theoretical expectations where the dependence of the strange baryon yields is expected to be linear with $\langle N_{part} \rangle$ for $\langle N_{part} \rangle \gtrsim 20$. One explanation for this deviation from the theory is that the volume responsible for strangeness production is not linearly proportional to the geometrical overlap region, as assumed in the model. A model that gives a reasonable description of the magnitudes and shapes of the enhancements with respect to centrality is described in [17]. This model allows for an over-saturation of strange quarks, which varies with centrality, and thus does not invoke chemical equilibration.

Fig. 1 is an average measurement of the difference in production between nucleus-nucleus and nucleon-nucleon collisions. Since the p_T distributions of the particles are approximately exponential these results are dominated by the physics occurring at $p_T \lesssim 2$ GeV/c. Differences in the p_T distributions for $p+p$ and Au+Au data are studied by calculating the nuclear modification factor:

$$R_{AA}(p_T, i) = \frac{d^2 N^{AA}(i)/dp_T dy}{T_{AA} d^2 \sigma^{NN}(i)/dp_T dy}, \quad (2)$$

$T_{AA} = \langle N_{bin} \rangle / \sigma_{inel}^{NN}$. Fig. 2a shows R_{AA} for Λ and the sum $\Xi^- + \bar{\Xi}^+$ for 0-5% Au+Au collisions along with those for inclusive $p+\bar{p}$ measurements [18, 19].

A striking feature of Fig. 2 is that both the central (top panel) and peripheral (bottom panel) R_{AA} distributions for the Λ and $\Xi^- + \bar{\Xi}^+$ reach maxima that are much greater than unity, a value that would signify binary collision scaling. In fact the peripheral collision R_{AA} distributions for the hyperons, Fig. 2b, are of approximately

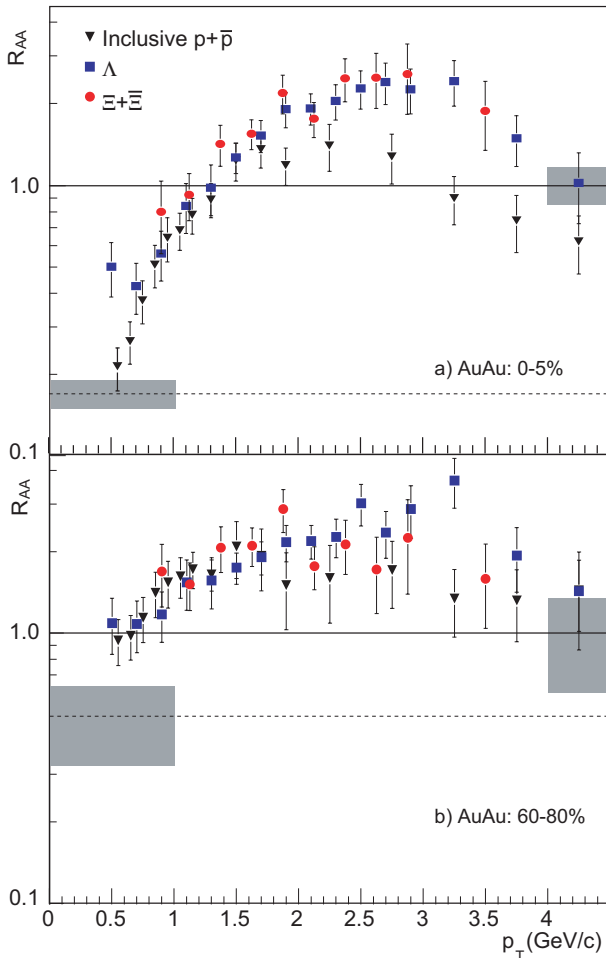


FIG. 2: (Color Online) R_{AA} from a) 0-5% and b) 60-80% central Au+Au events for $p+\bar{p}$ [18, 19], Λ and $\Xi^-+\bar{\Xi}^+$. Errors shown are statistical plus systematic added in quadrature. The band at unity shows the systematical uncertainty on $\langle N_{bin} \rangle$. The dashed line below unity shows the expected value of R_{AA} should the yields scale with $\langle N_{part} \rangle$ and the band around it shows the systematic uncertainty on $\langle N_{part} \rangle$.

the same magnitude as the central R_{AA} data, Fig. 2a, at intermediate to high p_T . These results are in contrast to the earlier reported suppression of high p_T hyperons observed via R_{CP} [5, 19, 20, 21], these data are reproduced in Fig. 3.

$$R_{CP}(p_T, i) = \frac{[d^2 N^{cent}(i)/dp_T dy / \langle N_{bin}^{cent} \rangle]}{[d^2 N^{periph}(i)/dp_T dy / \langle N_{bin}^{periph} \rangle]}, \quad (3)$$

Non-strange hadrons reveal a similar suppression when using $p+p$ or peripheral Au+Au collisions as a reference. For $p_T > 1.5$ GeV/c, unidentified charged hadrons show a suppression of the Au+Au spectra [7]. Comparing R_{AA} , Fig. 2, to R_{CP} , Fig. 3, shows that $R_{AA}(\Lambda) \approx R_{AA}(\Xi) \neq R_{AA}(p)$ but that $R_{CP}(\Lambda) \approx R_{CP}(\Xi) \approx R_{CP}(p)$, especially at intermediate to high p_T . This is possibly

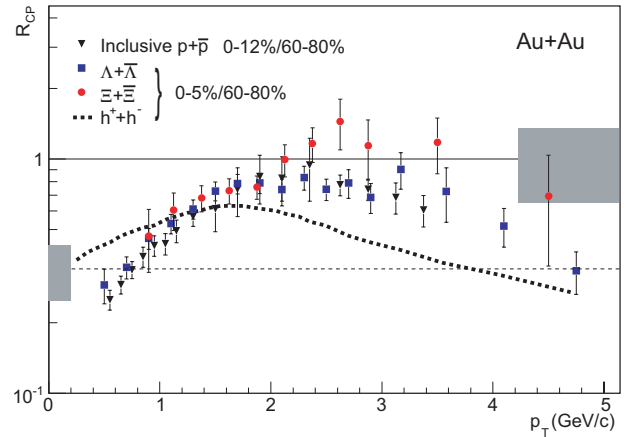


FIG. 3: (Color online) R_{CP} Au+Au events for $p+\bar{p}$ 0-12%/60-80% [19], $\Lambda+\bar{\Lambda}$ and $\Xi^-+\bar{\Xi}^+$ 0-5%/60-80% [5]. Also shown as the dashed curve are the results for h^++h^- for 0-5%/60-80% [20]. Errors shown are statistical plus systematic added in quadrature. The band at unity shows the systematical uncertainty on $\langle N_{bin} \rangle$. The dashed line below unity shows the expected value of R_{CP} should the yields scale with $\langle N_{part} \rangle$ and the band around it shows the systematic uncertainty on $\langle N_{part} \rangle$.

due to phase space effects in the $p+p$ data extending to this intermediate p_T regime. It is surprising that this decreased production in $p+p$ events, while predicted in the soft physics/thermal production regime, i.e. $p_T < 2$ GeV/c, extends out to, and even dominates in, this intermediate p_T region. Fig. 2a suggests that this effect is strong out to $p_T \sim 3$ GeV/c. The shapes of the R_{CP} distributions at intermediate to high p_T are generally interpreted as the result of parton energy loss in the hot dense matter and quark coalescence during hadronization. A comparison of Fig. 2a and Fig. 2b shows that the turnover points occur at approximately the same p_T . These data suggest that an enhancement of strangeness production has already set in in peripheral Au+Au collisions. This behavior is similar to that observed for the total yields in Fig. 1, and quantitatively consistent with expectations from canonical suppression in $p+p$. Some portion of the R_{AA} peak may be explained via the Cronin effect, the observed increase in intermediate p_T spectra in p -A collisions [22]. However, the Cronin enhancement stays constant, or possibly increases, as a function of centrality [23], and this is not seen in our data. Effects due to radial flow in the Au+Au data are significant at RHIC energies, even for the multi-strange baryons [24], but flow dominates only at low p_T . The shapes of the R_{AA} distributions below 1 GeV/c are markedly different. The peripheral collision data indicate approximate binary scaling of the baryon yields while the most central data fall beneath binary scaling but significantly above that suggesting participant scaling. This again indicates

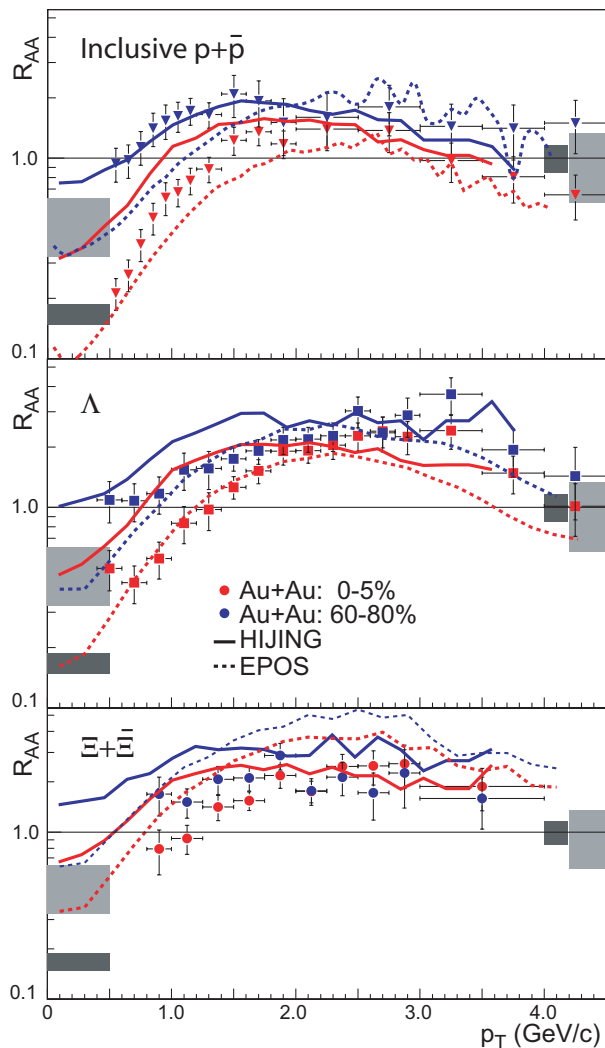


FIG. 4: (Color online) Comparison of R_{AA} from data to HIJING [27] and EPOS [29] for 0-5% and 60-80% most central Au+Au collisions, for $p+\bar{p}$, Λ and $\Xi^- + \bar{\Xi}^+$. Errors shown are statistical plus systematic added in quadrature. The bands at unity shows the systematical uncertainty on $\langle N_{bin} \rangle$. The bands below unity on the left of the graphs are centered at the expected value of R_{AA} should the yields scale with $\langle N_{part} \rangle$ and the widths of the bands indicate the systematic uncertainty on $\langle N_{part} \rangle$.

that there are different constraints on baryon production when going from $p+p$ to peripheral to central Au+Au collisions.

Comparisons to dynamical models can be used to understand in more detail how the close-to-equilibrium strangeness production can be achieved and whether the same mechanisms affect strange particle production at intermediate p_T . In the HIJING model [25] the yields and qualitative features of the strange baryon R_{AA} measurements (solid curves in Fig. 4) can only be obtained when baryon junctions and color strings are included [26, 27].

EPOS calculations [28, 29] (dashed curves in Fig. 4) produce similarly large differences in the hyperon R_{AA} and R_{CP} [28] to those measured at RHIC and also give a qualitatively reasonable representation of the shape of the data. EPOS describes particle production via a parton model where Au+Au collisions are represented as many binary interactions. Each binary interaction is described by a longitudinal color field which is expressed as a relativistic string, or parton ladder. At a very early proper time, before hadronization, the collision region is split into two environments, the core, in which the density of strings is high, and the corona, which surrounds the core and has a low string density. Production from the corona is due to collisions of nucleons at the periphery of the nuclei and modeled via string fragmentation. Corona production is thus similar to that from $p+p$ collisions. Meanwhile particle production from the core is approximated via a simple statistical hadronization process, similar to that described in [30], a collective flow profile is then imposed upon these particles. The relative weight of core to corona production varies with both centrality and particle species with the core dominating production in the most central events. Strange baryons are dominated by core production even in peripheral events.

In summary, we observe enhanced strange baryon mid-rapidity production in Au+Au collisions, especially in the more central events, when compared to the $\langle N_{part} \rangle$ scaled $p+p$ data from the same energy. The measured yields fail to scale with $\langle N_{part} \rangle$ as predicted if the GC regime is reached and the particle production volume scales with the geometrical overlap region. The magnitudes of the suppressions are different to those predicted, but close to those measured at SPS energies. At intermediate p_T the R_{AA} values are higher than binary scaling of $p+p$ data would predict. When attempting to understand the evolution of strange particle production from $p+p$ to central Au+Au one must take into account both the effects due to a suppression of strangeness production in $p+p$ and jet quenching plus quark recombination in Au+Au collisions, with the former dominating at intermediate p_T . Since the measured R_{CP} values for all strange baryons equal those of the inclusive protons in the intermediate and high p_T regions, and are significantly below binary scaling, the $p+p$ -like suppression is already predominantly removed in peripheral Au+Au collisions.

We thank the RHIC Operations Group and RCF at BNL, and the NERSC Center at LBNL and the resources provided by the Open Science Grid consortium for their support. This work was supported in part by the Offices of NP and HEP within the U.S. DOE Office of Science; the U.S. NSF; the BMBF of Germany; CNRS/IN2P3, RA, RPL, and EMN of France; EPSRC of the United Kingdom; FAPESP of Brazil; the Russian Ministry of Sci. and Tech.; the Ministry of Education and the NNSFC of China; IRP and GA of the Czech Republic, FOM of the Netherlands, DAE, DST, and CSIR of the Government of

India; Swiss NSF; the Polish State Committee for Scientific Research; Slovak Research and Development Agency, and the Korea Sci. and Eng. Foundation.

-
- [1] J. Rafelski and B. Müller, Phys. Rev. Lett. **48**, 1066 (1982).
- [2] J. Cleymans, K. Redlich and E. Suhonen, Z. Phys. **C 51**, 137 (1991). K. Redlich and A. Tounsi, Eur. Phys. J. **C24** 589 (2002).
- [3] F. Becattini, G. Pettini, Phys. Rev. **C 67**, 015205 (2003).
- [4] E. Andersen *et al.* (WA97), Phys. Lett. **B 449**, 401 (1999). F. Antinori *et al.* (WA97/NA57), Nucl. Phys. **A 698**, 118c (2002).
- [5] J. Adams *et al.* (STAR), Phys. Rev. Lett. **98**, 062301 (2007).
- [6] F. Antinori *et al.* (NA57) J. Phys. **bf G 32**, (2006) 427.
- [7] I. Aresene *et al.* (BRAHMS), Phys. Rev. Lett. **91**, 072305 (2003). S.S. Adler *et al.* (PHENIX), Phys. Rev. **C 69**, 034910 (2004). B.B. Back *et al.* (PHOBOS), Phys. Lett. **B 578**, 297 (2004). J. Adams *et al.* (STAR), Phys. Rev. Lett. **91**, 172302 (2003).
- [8] M. Gyulassy and M. Plumer, Phys. Lett. **B243** 432 (1990); R. Baier *et al. ibid.*, **345**, 277 (1995).
- [9] X.N. Wang and M. Gyulassy, Phys. Rev. Lett. **68** 1480 (1992); X.N. Wang, Phys. Rev. **C 58**, 2321 (1998).
- [10] K.H. Ackermann *et al.* (STAR), Nucl. Phys. **A 661**, 681c (1999).
- [11] B.I. Abelev *et al.* (STAR), in print PRC. nucl-ex/0607033.
- [12] J. Adams *et al.* (STAR), Phys. Rev. Lett. **92**, 112301 (2004).
- [13] R.J. Glauber, Lectures on Theoretical Physics, Vol. 1, p 315 (1959).
- [14] J. Adams *et al.* (STAR), Phys. Rev. **C 70**, 054907 (2004).
- [15] B.A. Cole *et al.* (E910), Phys.Lett. **B 639**, 210 (2006).
- [16] K. Redlich private communication, method described in [2].
- [17] J. Letessier and J. Rafelski, Phys. Rev. **C 73**, 014902 (2006).
- [18] J. Adams *et al.* (STAR), Phys. Lett. **B 637**, 161 (2006).
- [19] B.I. Abelev *et al.* (STAR), Phys. Rev. Lett. **97**, 152301 (2006)
- [20] J. Adams *et al.* (STAR), Phys. Rev. Lett. **91**, 172302 (2003).
- [21] S.S. Adler *et al.* (PHENIX), Phys. Rev. **C 69**, 034909 (2004). J. Adams *et al.* (STAR), Phys. Rev. Lett. **92**, 052302 (2004).
- [22] J.W. Cronin *et al.*, Phys. Rev. Lett. **31**, 1426 (1973); J.W. Cronin *et al.*, Phys. Rev. **D 11**, 3105 (1975).
- [23] J. Adams *et al.* (STAR), Phys. Lett. **B 616**, 8 (2005).
- [24] J. Adams *et al.* (STAR), Phys. Rev. Lett. **92**, 182301 (2004).
- [25] V. Topor Pop *et al.*, Phys. Rev. **C 70**, 064906 (2004) and references therein. Phys. Rev. **C75**, 014904 (2007).
- [26] V. Topor Pop, M. Gyulassy, J. Barrette, C. Gale, Phys. Rev. **C 72**, 054901 (2005).
- [27] V. Topor Pop *et al.*, Phys. Rev. **C 75**, 014904 (2007).
- [28] K. Werner, F. Liu and T. Pierog, J. Phys. **G 31**, S985 (2005). K. Werner, hep-ph/0603064.
- [29] K. Werner, Phys. Rev. Lett. **98**, 152301 (2007).
- [30] J. Rafelski, M. Danos, Phys. Lett. **B97** 279 (1980); P. Braun-Munzinger, I. Heppe, J. Stachel, Phys. Lett **B465** 15 (1999); J. Rafelski, J. Letessier, J. Phys. **G: Nucl. Part. Phys.** **28** 1819F (2002); F. Becattini, J. Manninen, M. Gazdzicki, Phys. Rev. **C73** 044905 (2006); J. Cleymans, H. Oeschler, K. Redlich, S. Wheaton, Phys. Rev. **C73** 034905 (2006).